Oral Reference: ICF100267OR

IN-SITU CHARACTERIZATION OF MATRIX RESPONSE TO FIBER FRACTURES

Jay C. Hanan[1], Irene J. Beyerlein [2], Ersan Üstündag[1], Geoffrey A. Swift[1]
Bjørn Clausen[1], Donald W. Brown[2], and Mark A. M. Bourke[2]

[1] *Department of Materials Science, California Institute of Technology, Pasadena, CA 91125, USA*
[2] *Materials Science and Technology Division, Los Alamos National Laboratory, Los Alamos, NM 87545, USA*

ABSTRACT

Successful application of metal matrix composites often requires strength and lifetime predictions that account for the deformation of each constituent. However, the deformation of individual phases in composites usually differs significantly from their respective monolithic behaviors. For instance, generally little is known about the *in-situ* deformation of the metal matrix and fiber/matrix interface region, other than that it likely differs from the bulk material response. This article describes an approach to quantifying the *in-situ* deformation parameters using neutron diffraction measurements of matrix failure around a fiber fracture in a model composite consisting of an Al matrix and a single Al_2O_3 fiber. We also study the shear sliding resistance as it evolves through fiber fracture upon loading and unloading. Matching the stress/strain distributions predicted from micromechanical models to the measured strain distributions determined by neutron diffraction under applied tensile loading results in an estimate of the typically non-linear, stress-strain behavior of the metal matrix.

KEYWORDS

Metal-matrix composite, neutron diffraction, constitutive behavior, fiber fracture, matrix yielding, Al-Al_2O_3 composite, interface shear strength.

INTRODUCTION

The strength and lifetime of fiber composites are largely governed by the nucleation and interaction of fiber fractures. These fractures unload onto neighboring fibers and matrix, generating strain concentrations which can promote more fiber breaks. The magnitudes and length scales of the strain concentration fields depend on the response of the matrix and interface. Therefore, knowledge on the *in-situ* constitutive behavior of these regions are crucial for determining internal stress states.

Particularly for metal matrix composites (MMCs), the deformation of the matrix material *in-situ* often differs significantly from its respective monolithic, bulk behavior. Generally little is known about the *in-situ* deformation behavior of the metal matrix and fiber/matrix interface region, other than that it likely differs from the bulk material response. There are many possible reasons: (i) microstructural constraints, (ii) localized strain gradients (e.g., near phase boundaries and defects), and (iii)

microstructural features, such as grain size and dislocation densities, of the matrix and interphase, that differ from monolithic features by virtue of the fabrication and consolidation process. The objective of this work is to develop *in-situ* constitutive laws for the matrix and the interface region.

Both single and multiple fiber micromechanical composite models for stress distributions around fiber fracture(s) employ various mathematical forms for the matrix or interface, ranging from rigid plastic to strain hardening, for instance. The simplest model, developed by Kelly and Tyson [1], assumes the matrix or interface deform only in shear and are rigid plastic with a constant shear stress τ_0. The fiber remains elastic and sustains only axial strains. Due to the high shear stress generated in the matrix next to the fracture site, inelastic matrix or interface deformation is assumed to initiate at the fiber fracture site and propagate axially away from the break. The axial length of this inelastic zone is commonly referred to as the slip length, L_s. For an MMC system, perhaps a less reasonable assumption is that axial deformation of the matrix is prohibited. According to [1], slip length L_s is

$$L_s = \frac{DE_f \varepsilon}{4\tau_0} \tag{1}$$

where, D is the fiber diameter, E_f is the Young's modulus of the fiber and ε is the far-field applied strain. The fiber axial coordinate z originates at the fiber fracture. For $z < L_s$ the fiber axial strain is simply ε, but for $z > L_s$ the fiber axial strain ε_f is

$$\varepsilon_f = \frac{4\tau_0 z}{DE_f} \tag{2}$$

This article describes a general approach to quantifying the *in-situ* deformation parameters by linking micromechanical modeling to neutron diffraction measurements of fiber and matrix strain around a fiber fracture. The model fiber composite studied consists of an Al matrix and a single Al_2O_3 fiber. The propagation and relaxation of matrix plasticity induced by the fiber fracture upon loading and unloading is also examined. To illustrate the approach we apply the Kelly-Tyson model [1] to the data. Matching the fiber axial stress distribution predicted from this model in Equation 2 to the neutron measured fiber strains under small applied load increments results in an estimate of the typically non-linear stress-strain behavior of the matrix.

EXPERIMENTAL PROCEDURE

A model composite comprised of a single, polycrystalline Al_2O_3 (alumina) fiber (4.75 mm diameter, from Coors Ceramics, Golden, CO) and an Al alloy (6061, ESPI Metals, Agoura Hills, CA) matrix prepared by casting was used in this study. In order to engineer fiber fracture at the center of the gage section a 0.7 mm thick notch was cut around the circumference of the fiber to a depth of 1 mm using a diamond saw. Prior to casting, the 6061 Al was machined to fit loosely in the mold around the fiber. The sample was cast in a stainless steel mold under vacuum after purging the mold with argon gas. The mold was machined to hold the alumina fiber vertically in a tube furnace while the Al melted around the fiber. Following 30 minutes at 800°C, the entire mold was quenched to room temperature in water. Cylindrical tensile samples were then machined from the cast. The final dimensions of the sample gave a 30 mm long gage length with an 8.23 mm total diameter. X-ray radiography images revealed a continuous matrix with no voids after casting. Reference samples (nominally free of thermal residual stresses) of the matrix and fiber were also prepared using the same technique. For the reference fiber sample, the Al matrix was polished away from the fiber along a 14 mm gage section in order to relieve the thermal residual stresses.

The mechanical behavior of the monolithic Al matrix was determined in tension using a screw-driven Instron load frame at a constant applied strain rate of 0.1 mm/min. The yield stress obtained by finding

the location on the stress/strain curve where it deviates from linear elastic behavior was 75 MPa. On the other hand, the 0.2% offset yield stress was found to be 89 MPa.

The neutron diffraction (ND) experiment was performed on the Neutron Powder Diffractometer (NPD) at the Los Alamos Neutron Scattering Center (LANSCE). Using a hydraulic load frame, the sample was loaded in tension in the presence of the neutron beam as shown in Fig. 1. Data were collected in 20 MPa intervals for approximately one hour at each step. Strain was measured on the sample using an extensometer with a 25 mm gage length. In addition, phase specific elastic strain was determined from the diffraction data via the Rietveld method [2,3]. A 10 mm wide neutron beam struck the entire width of the sample at an angle of 45° resulting in a 14 mm gage length (Fig. 1). Diffraction patterns were collected at $+90^{o}$ and $-90°$ 2θ providing strain information in both the longitudinal and transverse directions.

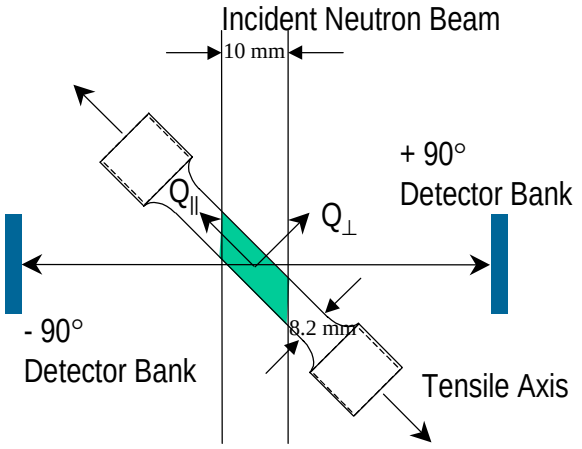

Figure 1. Schematic of the NPD tensile testing geometry. Specimen is at 45° to the incident beam. The scattering (Q) vectors for each detector bank indicate the directions of measured strains.

RESULTS AND DISCUSSION

Neutron Diffraction Measurements

Figs. 2-3 show the applied composite stress vs. axial (longitudinal) strain measured in each phase using ND. Within the error of the ND measurements (±150 με when specimens are changed and ±25 με during a single measurement), the thermal residual strains due to the mismatch of the thermal expansion coefficients of the fiber and the matrix were determined to be roughly relaxed. The reference values for the strains in Figs. 2-3 were taken to be the values measured from the monolithic ("stress-free") versions of the constituents. In other words, the data presented here include the (nearly relaxed) thermal residual strains.

Results shown in Fig. 2 suggest plastic deformation in the matrix during the first loading cycle at an applied composite stress around 60 MPa. A jump in the position of the load frame crosshead at around 55 MPa confirms the fiber broke during the first loading cycle. In addition, the plasticity observed from the extensometer (these data are not shown here) supports an assumption of discontinuity in the fiber, as does the change in slope after 60 MPa for both the fiber and matrix. Upon unloading, residual tensile strain is observed in the fiber and residual compressive strain is seen in the matrix. This is likely a result of the development of plastic strains in the matrix. Subsequent X-ray radiography showed separation of the fiber at the notch, which was not observed before loading.

In Fig. 2, we see further development of tensile residual strains in the fiber and compressive residual strains in the matrix upon fully unloading after each cycle. We suspect that propagation of localized matrix plastic deformation (around the fiber break) is largely responsible for these residual strains. Furthermore, there is a noticeable change in the composite modulus upon loading and unloading during

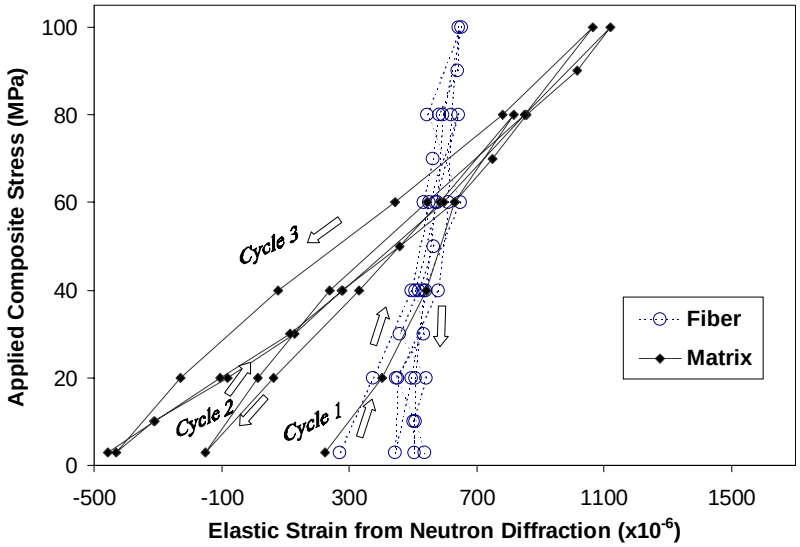

Figure 2. *Axial* strains measured by neutron diffraction in each phase vs. applied composite stress during loading/unloading cycles 1-3.

these first three cycles. For the loading portion of the first cycle, the modulus of the composite is about 156 GPa, nearly the value predicted by the rule of mixtures (~158 GPa). When the sample was unloaded, the composite modulus dropped to about 120 GPa. The modulus dropped again in the second loading cycle by 10 GPa and during the second unloading settled to about 74 GPa (approximately the modulus of the monolithic form of the matrix). The continuous decrease in the composite modulus suggests not only plastic deformation in the matrix, but some fiber pullout as well. In fact, X-ray radiography measurements performed after the ND experiment showed a fiber displacement of 0.15 mm along the axis at the notch. In addition, after completing the cycles, a plastic deformation zone was clearly visible at the surface of the sample in the position of the initial notch.

When Fig. 2 is compared with Fig. 3, marked differences between cycles 1-3, particularly for the matrix, and no significant changes during cycles 3-5 are observed. It is likely that by cycles 3-5, the plastic deformation in the matrix progressed outside the gage section. During the fifth loading/unloading cycle, the sample failed at a final load of 100 MPa after reaching a maximum load of 116 MPa. The matrix failed near the shoulder of the threaded section of the specimen and outside the section sampled by ND. At the failure plane, the fiber remained intact and pulled out of the threaded

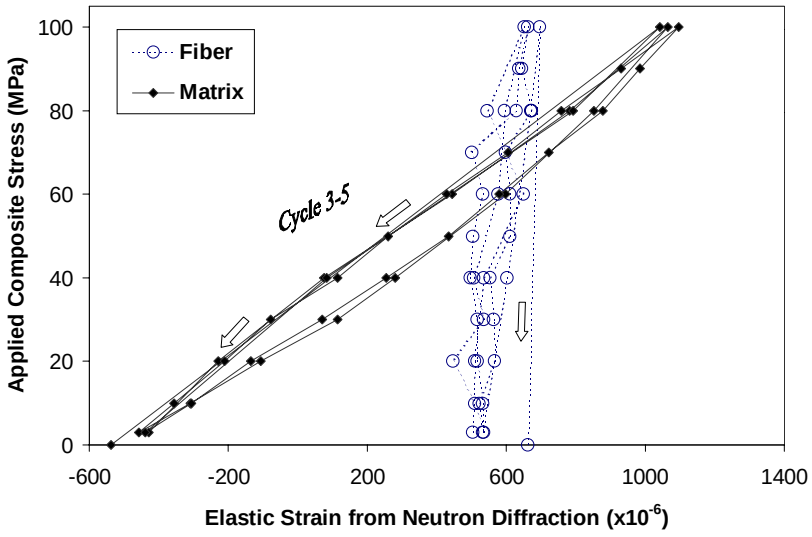

Figure 3. *Axial* strains measured by neutron diffraction in each phase vs. applied stress during loading/unloading cycles 3-5.

end leaving the middle of the gage section intact. The sample was maintained in position after the matrix failure and final residual strain values were recorded: +660 με in the fiber and –540 με in the matrix.

Comparison of Experimental Results with Modeling Predictions

Elastic axial fiber strain data from ND can be used to infer the elastic-plastic deformation response of the matrix. As discussed above, the ND results suggest localized plastic deformation in the matrix around the fiber break. This deformation will alter the elastic strain distribution in the fiber as predicted in several single and multifiber composite models. For instance, we use the simple shear-sliding model presented in [1] for the fiber strain due to a break in a single fiber composite and compare it with the ND data. We find that the slip length, L_s is usually greater than the gage length, z_{max} = 7 mm, at the maximum load of each cycle. Accordingly, Equation 2, when averaged over the length z_{max}, provides a relationship between an average axial fiber strain and the rigid plastic sliding resistance τ_0. This comparison suggests τ_0 varies from 22 to 25 MPa with each cycle when evaluated at its maximum load (Fig. 4). In Fig. 4, the values of applied stress where L_s was less than z_{max} were excluded. The τ_0 values are substantially different than the monolithic shear yield stress of 6061 Al (37 MPa). Such differences between bulk and *in-situ* metal matrix behavior were also observed in Al-Al_2O_3 multifiber composites [4]. Clearly the predicted parameters for *in-situ* matrix parameters depend on the constitutive models used for the fiber and matrix and composite stress analysis. The fact that τ_0 varies significantly during the loading/unloading cycles applied on the specimen suggests that the Kelly-Tyson model is inadequate in describing the behavior of the composite. Current work involves applying other micromechanical models for the matrix constitutive response to interpret the ND results and to obtain better representations of the *in-situ* constitutive behavior of the matrix.

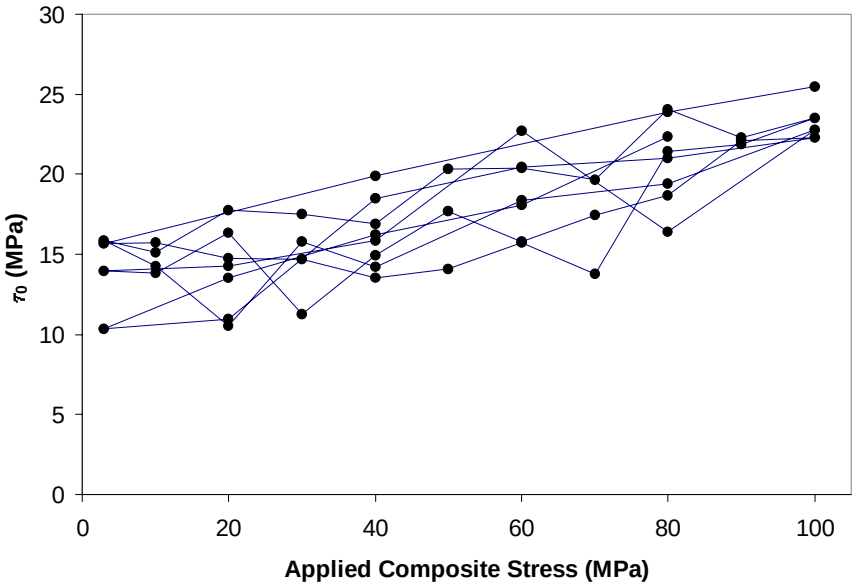

Figure 4. Variation of interface shear strength, τ_0 during loading/unloading cycles as a function of applied composite stress.

CONCLUSIONS

In this study, we examined the consequences of fiber fracture and localized matrix propagation under cyclic loading on the *in-situ* fiber and matrix strains. Even though the matrix fiber bond is strong, after the fiber fracture, the fiber carries only a small fraction of the total load. Plastic deformation in the matrix is observed immediately following fiber failure and increases with increasing applied load. The

shear sliding resistance, τ_0, which is about 30% smaller than the bulk shear yield stress, increases with each cycle.

ACKNOWLEDGEMENTS

This study was supported by the National Science Foundation (CAREER grant no. 9985264) at Caltech and a Laboratory-Directed Research and Development Project (no. 2000043) at Los Alamos. It also benefited from the national user facility at the Lujan Center, LANSCE, supported by the Department of Energy under contract W-7405-ENG-36.

REFERENCES

1. Kelly, A. and Tyson, W., (1965) *J. Mech. Phys. Solids*, 13, 329.
2. Larson, A. C. and von Dreele, R. B., *GSAS-General Structure Analysis System*, LAUR 86-748, Los Alamos National Laboratory, 1986.
3. Rietveld, H. M., (1969) *J. Appl. Cryst*., 2, 65.
4. He, J., Beyerlein, I. J. and Clarke, D. R., (1999) *J. Mech. Phys. Solids*, 47, 465.